Quantitative Analysis of the Chiral Amplification in the Amino Alcohol-Promoted Asymmetric Alkylation of Aldehydes with Dialkylzincs

Masato Kitamura, Seiji Suga, Hiromasa Oka, and Ryoji Noyori*

Contribution from the Department of Chemistry and Research Center for Materials Science, Nagoya University, Chikusa, Nagoya 464-8602, Japan

Received May 19, 1998

Abstract: Asymmetric reaction of dimethylzinc and benzaldehyde in the presence of (2*S*)-3-*exo*-(dimethylamino)isoborneol [(2*S*)-DAIB] exhibits unusual nonlinear phenomena. The enantiomeric purity of the product is much higher than that of the chiral source, DAIB, while the rate of the enantioselective catalysis decreases considerably as the enantiomeric excess (ee) of DAIB is lowered. Such effects originate from the reversible homochiral and heterochiral interaction of the coexistent enantiomeric zinc amino alkoxide catalysts which are formed from dimethylzinc and (2*S*)- and (2*R*)-DAIB. The thermodynamics of the five-component equilibration between the two monomers and three dimers, when coupled with the kinetics of the alkylation, strongly affects the extent of enantioselectivity and the reaction rate of the alkylation reaction. The overall profile of the nonlinear effects has been clarified mathematically using experimentally available parameters, viz., the equilibrium constants of the dimer/monomer conversion and the association of the monomeric catalyst with the organozinc and aldehyde, the rate constant of alkyl transfer from the catalyst/dimethylzinc/aldehyde mixed complex, the ee of DAIB, and the concentrations of DAIB, dimethylzinc, and aldehyde. 3D graphics are presented for the correlation of the enantiomeric purity of the product with DAIB ee and the concentrations of dimethylzinc and aldehyde and for the relationship between the reaction rate, DAIB ee, and the concentrations of the organozinc and aldehyde. The computer simulation is in good agreement with the experimental results, confirming that the nonlinear effects result from the competition of two enantiomorphic catalytic cycles involving the monomeric chiral zinc catalysts rather than the diastereomorphic catalytic cycles with dinuclear zinc catalysts. Furthermore, this study indicates that the degree of nonlinear effects in asymmetric catalysis could be affected not only by the catalyst ee but also by various reaction parameters, particularly the concentrations of the catalyst, reagent, and substrate as well as the extent of conversion.

In most asymmetric catalyses, the sense and extent of stereoselection are determined by the relative stabilities of the diastereomeric transition states in the first irreversible step.[1] In certain cases, however, the profile of asymmetric catalysis is highly affected by molecular interaction of the chiral catalyst with coexisting chiral or achiral molecules, and consequently, very unusual phenomena are seen.[2,3] A notable example is the amino alcohol-promoted asymmetric reaction of dialkylzincs and aldehydes that shows a remarkable nonlinear relation between the enantiomeric purities of the chiral source and the alkylation products.[4−9] Reaction of diethylzinc and benzaldehyde in toluene containing a small amount of (2*S*)-3-*exo*-(dimethylamino)isoborneol [(2*S*)-DAIB] in 15% ee (*S*:*R* = 57.5:42.5) affords after aqueous workup (*S*)-1-phenyl-1-propanol in 95% ee (*S*:*R* = 97.5:2.5), which is close to the 98% ee achieved with enantiomerically pure (2*S*)-DAIB.[5] Furthermore the reaction rate is highly dependent on the enantiomeric purity of the DAIB ancillary; the reaction aided by enantiomerically pure DAIB is much faster than that with racemic DAIB. The catalyst is considered to be a chiral tricoordinate alkylzinc amino alkoxide formed from diethylzinc and DAIB, which tends to dimerize in toluene. When the *S* and *R* catalysts coexist, both the homochiral interaction, giving *S*−*S* or *R*−*R*, and the heterochiral interaction leading to *S*−*R* are possible.[6] The dynamic monomer/dimer equilibrium coupled with the kinetics

(1) *Asymmetric Catalysis*; Bosnich, B., Ed.; Martinus Nijhoff Publishers: Dordrecht, 1986.

(2) Review: Noyori, R.; Kitamura, M. *Angew. Chem., Int. Ed. Engl.* **1991**, *30*, 49.

(3) Early reports on the nonlinear effect in asymmetric reactions: (a) Puchot, C.; Samuel, O.; Duñach, E.; Zhao, S.; Agami, C.; Kagan, H. B. *J. Am. Chem. Soc.* **1986**, *108*, 2353. (b) Agami, C.; Levisalles, J.; Puchot, C. *J. Chem. Soc., Chem. Commun.* **1985**, 441. (c) Agami, C. *Bull. Soc. Chim. Fr.* **1988**, 499. For the original works on discrimination between homo- and heterochiral pairs and nonlinear effects, see (for physical properties): Horeau, A. *Tetrahedron Lett.* **1969**, 3121. Horeau, A.; Guetté, J. P. *Tetrahedron* **1974**, *30*, 1923. (For asymmetric synthesis) Wynberg, H.; Feringa, B. *Tetrahedron* **1976**, *32*, 2831.

(4) (a) Noyori, R.; Suga, S.; Kawai, K.; Okada, S.; Kitamura, M. *Pure Appl. Chem.* **1988**, *60*, 1597. (b) Oguni, N.; Matsuda, Y.; Kaneko, T. *J. Am. Chem. Soc.* **1988**, *110*, 7877. (c) Bolm, C.; Schlingloff, G.; Harms, K. *Chem. Ber.* **1992**, *125*, 1191.

(5) (a) Kitamura, M.; Suga, S.; Kawai, K.; Noyori, R. *J. Am. Chem. Soc.* **1986**, *108*, 6071. (b) Noyori, R.; Suga, S.; Kawai, K.; Okada, S.; Kitamura, M.; Oguni, N.; Hayashi, M.; Kaneko, T.; Matsuda, Y. *J. Organomet. Chem.* **1990**, *382*, 19. The first catalytic asymmetric addition of diethylzinc to benzaldehyde: Oguni, N.; Omi, T. *Tetrahedron Lett.* **1984**, *25*, 2823.

(6) For the structural origin of differences between the homochiral and heterochiral dimers, see: Kitamura, M.; Yamakawa, M.; Oka, H.; Suga, S.; Noyori, R. *Chem. Eur. J.* **1996**, *2*, 1173.

(7) Kitamura, M.; Okada, S.; Suga, S.; Noyori, R. *J. Am. Chem. Soc.* **1989**, *111*, 4028.

(8) Kitamura, M.; Suga, S.; Niwa, M.; Noyori, R. *J. Am. Chem. Soc.* **1995**, *117*, 4832.

(9) Kitamura, M.; Suga, S.; Niwa, M.; Noyori, R.; Zhai, Z.-X.; Suga, H. *J. Phys. Chem.* **1994**, *98*, 12776.

S0002-7863(98)01740-5 CCC: $15.00
Published on Web 09/15/1998

of the catalysis results in the deviation of the *S*:*R* catalyst ratio from the original ratio of DAIB enantiomer and in turn the nonlinear phenomenon.[7−9] This article describes the quantitative analysis of the overall profile of stereoselectivity and the reaction rate of the amino alcohol-aided alkylation.

Kagan has done a mathematical analysis on a related, but different, case using the titanium tartrate-catalyzed oxidation of allylic alcohols and sulfides, where homochiral and heterochiral Ti catalysts are involved in the stereodetermining transition states.[3a,10,11] In these reactions, metal modification by a partially resolved chiral auxiliary results in the *irreversible*, nonstatistical formation of diastereomeric Ti complexes with two chiral auxiliary molecules of types ML^*_2 or $M_2L^*_2$ (M = metallic species; L* = chiral ligand). The differences in the stabilities and reactivities of the stereoisomers are believed to cause the nonlinear effect.[12] In contrast, the organozinc chemistry is characterized by the reversibility of the chiral recognition of the enantiomeric catalysts of type ML* as well as the involvement of a single chiral molecule in the stereodetermining transition state. Thus, the nonlinear effects of the Zn chemistry are based on the relative significance of *enantiomorphic catalytic cycles*, in contrast to the unusual phenomena of the Ti chemistry that arise from the competition of *diastereomorphic catalytic cycles*. This study aims to confirm this view. The present mathematical treatment, as a complement to Kagan's accomplishment,[3a,11] will help to deepen the understanding of the origin and mechanism of the nonlinear phenomena in various asymmetric catalysis.[3,4]

General Mathematical Treatment

We assume a disubstrate−monoproduct catalysis that follows the Michaelis−Menten-type kinetic law. Supposing that enantiomeric catalysts, *S* and *R*, are coexistent in the same reaction system ([*S*] ≥ [*R*]) and that there exists a dynamic equilibrium between the catalysts and the homochiral and heterochiral dimers, *S*−*S*, *R*−*R*, and *S*−*R*, as illustrated in the center of Scheme 1. The catalytically unreactive dimers dissociate into the reactive monomers with the given dissociate constants, K_{homo} and K_{hetero}.[9] Monomeric *S* and *R* assemble a reactant (Rea) and a substrate (Sub), with a given associate constant K_{assoc} to form the catalyst/reactant/substrate mixed complexes, *S*−Rea−Sub and *R*−Rea−Sub, which are converted with the same rate constant *k* to the catalyst/product complexes, *S*−P and *R*−P. Finally, the enantiomeric products, P_S and P_R, are released from these complexes by the action of Rea or Sub to complete the catalytic cycle. To establish a smooth catalytic cycle, all steps must proceed at a reasonable rate; inhibition by the reactant, substrate, or product should be avoided. The enantiomeric purity of the product, ee_P, limited by the enantioselectivity, ee_P^{max}, which may be obtained with the enantiomerically pure catalyst, is determined by the relative turnovers of the two enantiomorphic catalytic cycles.

Scheme 1[a]

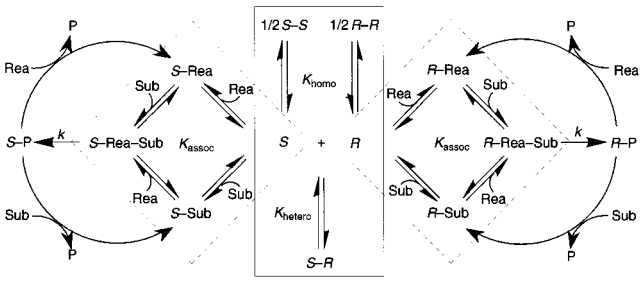

[a] P = product, P_R or P_S.

For mathematical purposes, a steady-state approximation is applied to the concentrations of *S*−Rea−Sub and *R*−Rea−Sub. These intermediates are irreversibly and stereoselectively converted to *S*−P or *R*−P, and the turnover of the catalytic cycles is limited by this step. Thus, when Rea and Sub exist in sufficient excess to the catalyst, the ee_P is determined by ee_P^{max} and the relative concentration of *S*−Rea−Sub to *R*−Rea−Sub. The initial reaction rate v_0 can be expressed by multiplication of the sum of [*S*−Rea−Sub] and [*R*−Rea−Sub] and the rate constant *k*. Equations 1 and 2 are thus established. Since the

$$ee_P = ee_P^{max}\frac{[S-Rea-Sub] - [R-Rea-Sub]}{[S-Rea-Sub] + [R-Rea-Sub]} \quad (1)$$

$$v_0 = k([S-Rea-Sub] + [R-Rea-Sub]) \quad (2)$$

total catalyst concentration, $[C_{tot}]$, is approximated by the sum of the concentrations of the chiral source existing before the rate-determining step as the monomeric catalysts, the dimers, and the Rea and Sub complexes, the enantiomeric purity of the chiral source, $ee_{C_{tot}}$, can be expressed by eq 3.

$$ee_{C_{tot}} = (([S] + 2[S-S] + [S-R] + [S-Rea-Sub] - ([R] + 2[R-R] + [S-R] + [R-Rea-Sub]))/[C_{tot}] \quad (3)$$

To correlate ee_P and v_0 with ee_{Ctot} using the equilibrium constants, K_{homo}, K_{hetero}, and K_{assoc}, and the concentrations of C_{tot}, Rea, and Sub,[13] the concentration terms of the dimers and catalyst/reactant/substrate complexes can be eliminated from eqs 1−3 by using eqs 4−6 and eq 7. Here for simplification, α

(10) Other asymmetric reactions showing nonlinear effects. (Sharpless epoxidation of geraniol or sulfide): Reference 3a. (Ene reaction): Terada, M.; Mikami, K. *J. Chem. Soc., Chem. Commun.* **1994**, 833. (Diels−Alder reaction): Iwasawa, N.; Hayashi, Y.; Sakurai, H.; Narasaka, K. *Chem. Lett.* **1989**, 1581. Mikami, K.; Motoyama, Y.; Terada, M. *J. Am. Chem. Soc.* **1994**, *116*, 2812. Kobayashi, S.; Ishitani, H.; Araki, M.; Hachiya, I. *Tetrahedron Lett.* **1994**, *35*, 6325. (Silylcyanation of benzaldehyde): Hayashi, M.; Matsuda, T.; Oguni, N. *J. Chem. Soc., Chem. Commun.* **1990**, 1364. (Conjugate addition of organometallics to α,β-unsaturated carbonyl compounds): Bolm, C.; Ewald, M.; Felder, M. *Chem. Ber.* **1992**, *125*, 1205. Tanaka, K.; Matsui, J.; Suzuki, H. *J. Chem. Soc., Perkin Trans. 1* **1993**, 153. Rossiter, B. E.; Eguchi, M.; Miao, G.; Swingle, N. M.; Hernández, A. E.; Vickers, D.; Fluckiger, E.; Patterson, R. G.; Reddy, K. V. *Tetrahedron* **1993**, *49*, 965. Zhou, Q.-L.; Pfaltz, A. *Tetrahedron* **1994**, *50*, 4467. de Vries, A. H. M.; Jansen, J. F. G. A.; Feringa, B. L. *Tetrahedron* **1994**, *50*, 4479. (Hajos−Wiechert intramolecular aldol reaction): References 3b and 3c. (Nitro-aldol reaction): Sasai, H.; Suzuki, T.; Itoh, N.; Shibasaki, M. *Tetrahedron Lett.* **1993**, *34*, 851. (Allylation of aldehydes using organotin compounds): Keck, G. E.; Krishnamurthy, D.; Grier, M. C. *J. Org. Chem.* **1993**, *58*, 6543. (Meerwein−Ponndorf−Verley reduction): Evans, D. A.; Nelson, S. G.; Gagné, M. R.; Muci, A. R. *J. Am. Chem. Soc.* **1993**, *115*, 9800. (Oxidation of sulfides): Komatsu, N.; Hashizume, M.; Sugita, T.; Uemura, S. *J. Org. Chem.* **1993**, *58*, 4529. (Reduction of acetophenone by diisopinocamphenyl chloroborate): Girard, C.; Kagan, H. B. *Tetrahedron: Asymmetry* **1997**, *8*, 3851.

(11) Guillaneux, D.; Zhao, S.-H.; Samuel, O.; Rainford, D.; Kagan, H. B. *J. Am. Chem. Soc.* **1994**, *116*, 9430. In the Kagan reservoir effect, catalytic species are considered to be preserved as their associates. See also: Blackmond, D. G. *J. Am. Chem. Soc.* **1997**, *119*, 12934.

(12) For the nonlinear effect based on the asymmetric activation of racemic catalysts, see: Matsukawa, S.; Mikami, K. *Tetrahedron: Asymmetry* **1997**, *8*, 815. Matsukawa, S.; Mikami, K. *Enantiomer* **1996**, *1*, 69. Mikami, K.; Matsukawa, S. *Nature* **1997**, *385*, 613. Ohkuma, T.; Doncet, H.; Pham, T.; Mikami, K.; Korenaga, T.; Terada, M.; Noyori, R. *J. Am. Chem. Soc.* **1998**, *120*, 1086.

(13) The initial concentrations of Rea and Sub approximate [Rea] and [Sub], because *S*−Rea−Sub and *R*−Rea−Sub are present only in small quantities.

$$K_{homo} = \frac{[S]^2}{[S{-}S]} = \frac{[R]^2}{[R{-}R]} \quad (4)$$

$$K_{hetero} = \frac{[S][R]}{[S{-}R]} \quad (5)$$

$$K_{assoc} = \frac{[S{-}Rea{-}Sub]}{[S][Rea][Sub]} = \frac{[R{-}Rea{-}Sub]}{[R][Rea][Sub]} \quad (6)$$

$$[C_{tot}] = [S] + 2[S{-}S] + [S{-}R] + [S{-}Rea{-}Sub] + [R] + 2[R{-}R] + [S{-}R] + [R{-}Rea{-}Sub] \quad (7)$$

and β are introduced, where $\alpha = [S] + [R]$ ($\alpha > 0$) and $\beta = [S][R]$ ($\beta \geq 0$). Modification of the two equations by assuming $[S] \geq [R]$ gives

$$[S] = (\alpha + \sqrt{\alpha^2 - 4\beta})/2 \quad (8)$$

$$[R] = (\alpha - \sqrt{\alpha^2 - 4\beta})/2 \quad (9)$$

As the equation $ee_P = ee_P^{max}([S] - [R])/([S] + [R])$ is established by substitution of eq 6 into eq 1, rearrangement with eqs 8 and 9 affords

$$ee_P = ee_P^{max}\sqrt{\alpha^2 - 4\beta}/\alpha \quad (10)$$

When eqs 4−6 are substituted into eq 3 to eliminate $[S{-}S]$, $[R{-}R]$, $[S{-}R]$, $[S{-}Rea{-}Sub]$, and $[R{-}Rea{-}Sub]$ followed by replacement of $[S]$ and $[R]$ using eqs 8 and 9 gives eq 11 in

$$ee_{C_{tot}} = \frac{(2\alpha/K_{homo}) + 1 + K_{assoc}[Rea][Sub]\sqrt{\alpha^2 - 4\beta}}{[C_{tot}]} \quad (11)$$

which ee_{Ctot} is related to K_{homo}, K_{assoc}, $[C_{tot}]$, [Rea], [Sub], α, and β. Combination of eq 7 with eqs 4−6, 8, and 9 followed by rearrangement for β establishes eq 12. Since β is expressed

$$\beta = \frac{-K_{hetero}(2\alpha^2 + \alpha K_{homo} - ([C_{tot}] - K_{assoc}[Rea][Sub]\alpha)K_{homo})}{2(K_{homo} - 2K_{hetero})} \quad (12)$$

as a function of α, ee_P is now given as a function of ee_{Ctot} through α by using K_{homo}, K_{hetero}, K_{assoc}, $[C_{tot}]$, [Rea], and [Sub] with a fixed ee_P^{max} value in a given asymmetric reaction. Once these constants are determined, the overall profile of stereoselectivity is defined by the five-component monomer/dimer equilibration of the chiral catalysts, bounded by solid lines in Scheme 1, and the reversible formation of the product-determining complexes, $S{-}Rea{-}Sub$ and $R{-}Rea{-}Sub$. Here, the conditions (1) $\alpha^2 - 4\beta > 0$, (2) $0 \leq ee_{Ctot} \leq 1$, and (3) $0 \leq ee_P \leq ee_P^{max}$ must be satisfied. The type and degree of nonlinearity in the ee_{Ctot}/ee_P relation is decided by the α range. The requirements of $0 \leq ee_{Ctot}$ and $0 \leq ee_P \leq ee_P^{max}$ are filled when $\alpha^2 - 4\beta > 0$, as seen from eqs 11 and 10, respectively. Substitution for β in the first inequality using eq 12 affords

$$\alpha^2 - 4\beta = ((K_{homo} + 2K_{hetero})\alpha^2 + 2K_{homo}K_{hetero}(1 + K_{assoc}[Rea][Sub])\alpha - 2K_{homo}K_{hetero}[C_{tot}])/(K_{homo} - 2K_{hetero}) > 0 \quad (13)$$

This equation shows that $K_{homo} = 2K_{hetero}$ is the branching condition which determines the type of nonlinearity. At this point, the enantiomer ratio of the catalyst molecules present in the whole system is identical to the $[S{-}Rea{-}Sub]$ to $[R{-}Rea{-}Sub]$ ratio, resulting in a linear relationship between ee_P and ee_{Ctot}. When K_{homo} becomes greater than $2K_{hetero}$, chirality of the product is amplified, and the denominator of eq 13 must be positive. Solving the second-order inequality 13 in combination with $ee_{Ctot} \leq 1$, the α ranges for the positive nonlinear effects are given in eq 14. The highest and the lowest α values are

$$(-K_{homo}(1 + K_{assoc}[Rea][Sub]) + (K_{homo}(8[C_{tot}] + K_{homo} + 2K_{homo}K_{assoc}[Rea][Sub] + K_{homo}K_{assoc}^2[Rea]^2[Sub]^2))^{1/2})/4 \geq \alpha \geq \left(K_{homo}K_{hetero}\left(\left((1 + K_{assoc}[Rea][Sub])^2 + 2[C_{tot}]\left(\frac{1}{K_{hetero}} + \frac{2}{K_{homo}}\right)\right)^{1/2} - (1 + K_{assoc}[Rea][Sub])\right)\right)/(K_{homo} - 2K_{hetero}) \quad (14)$$

reversed for the negative nonlinear effect. In addition, modification of eq 2 using eqs 6, 8, and 9 affords the rate eq 15.

$$\nu_0 = kK_{assoc}[Rea][Sub]\alpha \quad (15)$$

Now all the important variants ee_P, ee_{Ctot}, and ν_0 are described by the four or six factors through parameter α: $ee_P = f_1(K_{homo}, K_{hetero}, K_{assoc}, [C_{tot}], [Rea], [Sub], \alpha)$ as seen from eqs 10 and 12. $ee_{Ctot} = f_2(K_{homo}, K_{hetero}, K_{assoc}, [C_{tot}], [Rea], [Sub], \alpha)$ from eqs 11 and 12. $\nu_0 = f_3(k, K_{assoc}, [Rea], [Sub], \alpha)$ from eq 15.

The selectivity profile and the kinetic behavior of a given asymmetric reaction system can be clarified by graphical expression with the K_{homo}, K_{hetero}, and K_{assoc} values, which can be experimentally determined by spectroscopic methods, molecular weight measurement, and kinetic analysis. Six frames, a−f, in Figure 1 illustrate α-parametrically plotted curves derived from eqs 10−12 by changing four factors, K_{homo}:K_{hetero} ratio, $[C_{tot}]$, [Rea], and [Sub], and the association constant K_{assoc} using theoretical values for the other parameters. As the K_{homo}:K_{hetero} ratio decreases, the positive deviation diminishes and finally returns to linearity (frame a). After passing the $K_{homo} = 2K_{hetero}$ boundary, a negative nonlinearity begins to appear (frame b). Frames c−e predict that only a weak nonlinear effect will be observed with a very low $[C_{tot}]$, very high [Rea] and [Sub], and high association constants for catalyst *S* or *R*, Rea, and Sub. As seen from frame f, the extent of the positive nonlinear effect is enlarged when [Rea] and [Sub] are decreased from 1000 to 100 mM with the C_{tot}, Rea, and Sub ratio fixed to 1:50:50. A further decrease of concentrations, however, tends to diminish the nonlinear effect.

Figure 2 expresses graphically the influence of ee_{Ctot} as well as [Rea] and [Sub] on the reaction velocity. Substantial rate reduction is anticipated with the decrease of the enantiomeric purity of the catalyst. Increasing the K_{homo}:K_{hetero} ratio enhances the sensitivity. The concentrations of Rea and Sub affect the rate more strongly in the reaction using an enantiomerically pure catalyst ($ee_{Ctot} = 1$) than in the reaction with the racemic catalyst ($ee_{Ctot} = 0$). The velocity with an enantiopure catalyst is also more easily maximized than that with a racemic catalyst.

A Case Study: Amino Alcohol-Promoted Asymmetric Reaction of Dialkylzincs and Aldehydes. Dialkylzincs react with prochiral aldehydes in the presence of a catalytic amount of nonracemic DAIB to give, after hydrolysis, optically active secondary alcohols.[5] Frame a of Figure 3 illustrates the enantioselectivity observed in the reaction of dimethylzinc (DMZ) (420 mM) and benzaldehyde (BzH) (420 mM) in the presence of (2*S*)-DAIB (8 mM) in toluene at 40 °C. The

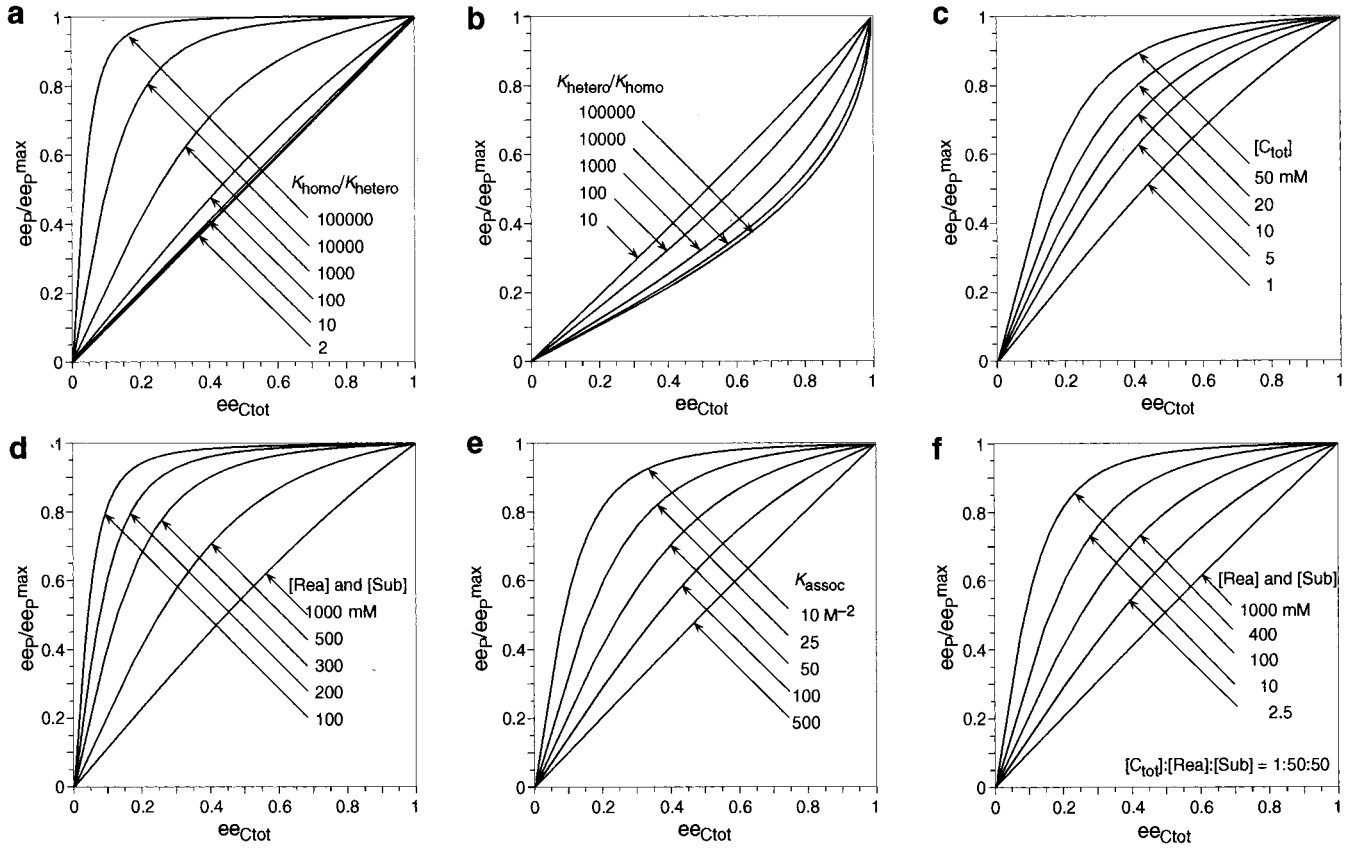

Figure 1. Simulation of the nonlinear relationship between ee_P and ee_{Ctot} in a theoretical asymmetric catalysis with the following parameters. a: $K_{homo} = 1.0 \times 10^{-2}$ M; $K_{assoc} = 5.0 \times 10^{1}$ M^{-2}; $[C_{tot}] = 10$ mM; [Rea] = [Sub] = 500 mM. b: $K_{homo} = 1.0 \times 10^{-2}$ M; $K_{assoc} = 5.0 \times 10^{1}$ M^{-2}; $[C_{tot}] = 10$ mM; [Rea] = [Sub] = 500 mM. c: $K_{homo} = 1.0 \times 10^{-2}$ M; $K_{hetero} = 1.0 \times 10^{-5}$ M; $K_{assoc} = 5.0 \times 10^{1}$ M^{-2}; [Rea] = [Sub] = 500 mM. d: $K_{homo} = 1.0 \times 10^{-2}$ M; $K_{hetero} = 1.0 \times 10^{-5}$ M; $K_{assoc} = 5.0 \times 10^{1}$ M^{-2}; $[C_{tot}] = 10$ mM. e: $K_{homo} = 1.0 \times 10^{-2}$ M; $K_{hetero} = 1.0 \times 10^{-5}$ M; $[C_{tot}] = 10$ mM; [Rea] = [Sub] = 500 mM. f: $K_{homo} = 1.0 \times 10^{-2}$ M; $K_{hetero} = 1.0 \times 10^{-5}$ M; $K_{assoc} = 5.0 \times 10^{1}$ M^{-2}.

enantiomeric purity of (*S*)-1-phenylethanol obtained at an early stage of reaction ranges from 95% with enantiomerically pure (2*S*)-DAIB to 0% with racemic DAIB, where the variation is not proportional to the enantiomeric purity of DAIB.[14] In addition, as shown in frame b, the reaction with enantiomerically pure DAIB proceeds ~6 times faster than with racemic DAIB. Thus, the rate depends on the enantiomeric purity of DAIB but the extent is not straightforward. The origin of these unusual phenomena has been explained qualitatively in terms of the enantiomer recognition of the asymmetric catalyst as outlined in Scheme 2.[6−9,11] The tricoordinate Zn complex **1**, which is in equilibrium with the dimer **2**, acts as catalyst of the enantioselective reaction of DMZ and BzH. When (2*S*)- and (2*R*)-**1** are coexistent, the homochiral and heterochiral dimerizations, leading to (2*S*,2′*S*)- and (2*R*,2′*R*)-**2** and (2*S*,2′*R*)-**2**, respectively, are possible, with the latter overwhelmingly favored. The higher stability of (2*S*,2′*R*)-**2** reduces the total amount of **1** and also causes its enantiomeric purity to deviate with the added DAIB auxiliary. As a consequence, substantial nonlinearity is seen for both the reactivity and enantioselectivity. We here analyze such effects quantitatively using experiments and computer simulation.

Equilibrium and Rate Constants. Scheme 2 consists of the five-component equilibration of the chiral catalysts, **1** ⇄ **2**, the formation of the **1**/DMZ/BzH mixed-ligand complex **3**, and the turnover-limiting alkyl transfer in **3**. (2*S*)-**3** produces (2*S*)-**4**[15] predominantly containing (*S*)-1-phenylethoxide (*S*:*R* = 97.5:2.5), while (2*R*)-**3** gives (2*R*)-**4** selectively.[15] The final product **4**, upon reaction with DMZ or BzH, affords tetrameric methylzinc 1-phenylethoxide (**5**), and a **1**/DMZ or **1**/BzH complex, respectively, and then **3** to establish the catalytic cycle. The formation of the stable tetrameric alkoxide **5** is important to minimize the undesired product inhibition. The two catalytic cycles are enantiomorphic. This mechanism is consistent with the experimental results[7] and the ab initio MO calculations.[16]

Seven parameters are required for the quantitative analysis of Scheme 2. Three of these, $[C_{tot}]$, [Rea], and [Sub], are defined arbitrarily as the concentrations of (2*S*)-DAIB, DMZ, and BzH, whereas the remaining key constants, K_{homo}, K_{hetero}, K_{assoc}, and k, are obtained experimentally.

The molecular weight measurement of stereoisomeric **2** by vapor pressure osmometry in toluene at 40 °C indicated that the homochiral and heterochiral dimers dissociate into catalytic **1** with dissociation constants, $K_{homo} = (3.0 \pm 1.0) \times 10^{-2}$ M and $K_{hetero} = 1 \times 10^{-5}$ M, respectively.[9] Thus, in a 10 mM toluene solution of (2*S*,2′*S*)- or (2*R*,2′*R*)-**2**, ~60% of the homochiral dimer is dissociated into the monomer, while, under the same conditions, the degree of dissociation of (2*S*,2′*R*)-**2** is only ~3%.

The rate constant k and the equilibrium constant K_{assoc} can be determined by kinetic experiments using enantiomerically pure DAIB. Figure 4a shows the initial rate as a function of the concentration of an equimolar mixture of DMZ and BzH.

(14) The optical yield of the reaction of DMZ and BzH using optically pure DAIB ranges from 91 to 95%. Use of freshly distilled DMZ gives the product in 95% ee.

(15) The molecular weight is unknown. Complex **4** may be in equilibrium with the dimer and other aggregates formed with coexisting organozinc complexes.

(16) Yamakawa, M.; Noyori, R. *J. Am. Chem. Soc.* **1995**, *117*, 6327.

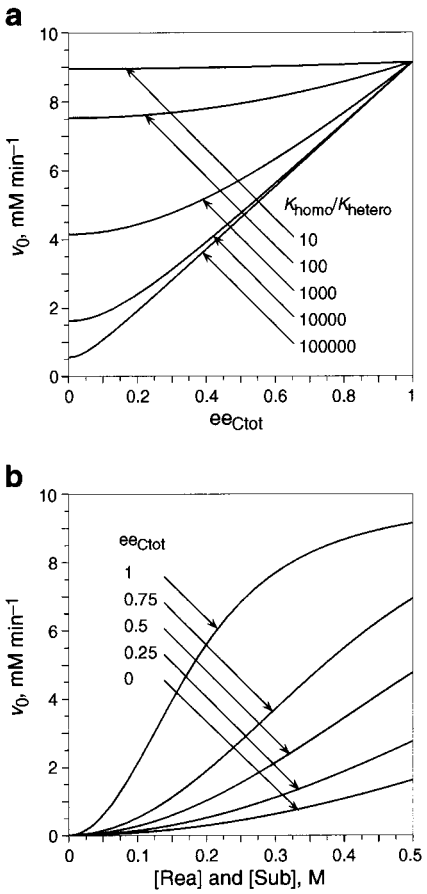

Figure 2. Graphical expression of the ν_0−ee$_{Ctot}$ relation (a) and the relation of ν_0 with [Rea] and [Sub] (b) in a theoretical asymmetric reaction with the following parameters. a: $K_{homo} = 1.0 \times 10^{-2}$ M; $K_{assoc} = 5.0 \times 10^{1}$ M^{-2}; $k = 1.0$ min^{-1}; [C_{tot}] = 10 mM; [Rea] = [Sub] = 500 mM. b: $K_{homo} = 1.0 \times 10^{-2}$ M; $K_{hetero} = 1.0 \times 10^{-6}$ M; $K_{assoc} = 5.0 \times 10^{1}$ M^{-2}; $k = 1.0$ min^{-1}; [C_{tot}] = 10 mM.

The reaction using an 8 mM solution of pure (2*S*)-DAIB in toluene at 40 °C proceeds with a zero-order kinetics in the reactant and substrate concentration when they are greater than 800 mM, although the rate depends on the concentration in a range of 0−800 mM. Thus, in the presence of a large excess of DMZ and BzH, (2*S*)-**1** is completely converted to (2*S*)-**3**, giving saturation kinetics. The maximal velocity, ν_0^{sat}, at this point is correlated with k and [C_{tot}] to give the equation $\nu_0^{sat} = k[C_{tot}]$, where [C_{tot}] corresponds to the concentration of DAIB since **1** is formed quantitatively from DAIB and DMZ. Thus the rate constant k of the (2*S*)-DAIB-promoted reaction is calculated to be 2.5×10^{-1} min^{-1} by using the observed velocity, $\nu_0^{sat} = 2.0$ mM min^{-1} and [C_{tot}] = 8 mM. The reaction using racemic DAIB did not attain saturation kinetics even with high concentrations of DMZ and BzH because of the high stability of (2*S*,2′*R*)-**2**. The association constant K_{assoc} is determined to be 2.0×10^{1} M^{-2} by curve-fitting between the observed kinetics (Figure 4a) and the simulated kinetics (Figure 4b) with K_{assoc} in the range of 5−100 M^{-2}.

Validity of the Mathematical Treatment. Methylation is normally conducted with [DAIB] ≤ 34 mM and [DMZ] = [BzH] < 840 mM. Figure 5 illustrates the graphic expression of the three-dimensional (3D) correlation between ee$_P$, ee of DAIB (ee$_{Ctot}$ in the general discussion), and [DMZ] and [BzH] (1:1 molar ratio), and between ν_0, DAIB ee, and [DMZ] and [BzH] (1:1 molar ratio). The curved surfaces of frames a−c have been obtained by simulation using the experimentally determined K_{homo}, K_{hetero}, K_{assoc}, and k where [C_{tot}] = [DAIB] = 8−34 mM. Frame a predicts that the ee$_P$ nonlinearly will increase with an increase of the ee value of DAIB when [DMZ] and [BzH] are fixed. With a fixed DAIB ee, the degree of nonlinearity is expected to decrease with an increase of [DMZ] and [BzH]. The surface of frame b denotes the reaction rate ν_0 calculated by varying ee$_{Ctot}$ and [DMZ] and [BzH] with [DAIB] = 8 mM. Frame c gives a simulated profile of the reaction with [DAIB] = 16 mM, suggesting rate enhancement by increasing [DAIB] from 8 to 16 mM and, particularly, [DMZ] and [BzH]. The ν_0−DAIB ee projected planes predict that the initial methylation rate is nonlinearly enhanced by increasing the ee value of DAIB, as expected from the **1** ⇄ **2** equilibration in favor of the heterochiral dimerization. In all cases, the computer-generated curves (lines) provide a good fit with the experimental results (dots) obtained at the early stage of the reaction, indicating the validity of the theoretical analysis. This confirms the mechanistic assumption as well; the nonlinear effects originate from competition of the two enantiomorphic catalytic cycles involving (2*S*)-**1** and (2*R*)-**1** under standard reaction conditions.

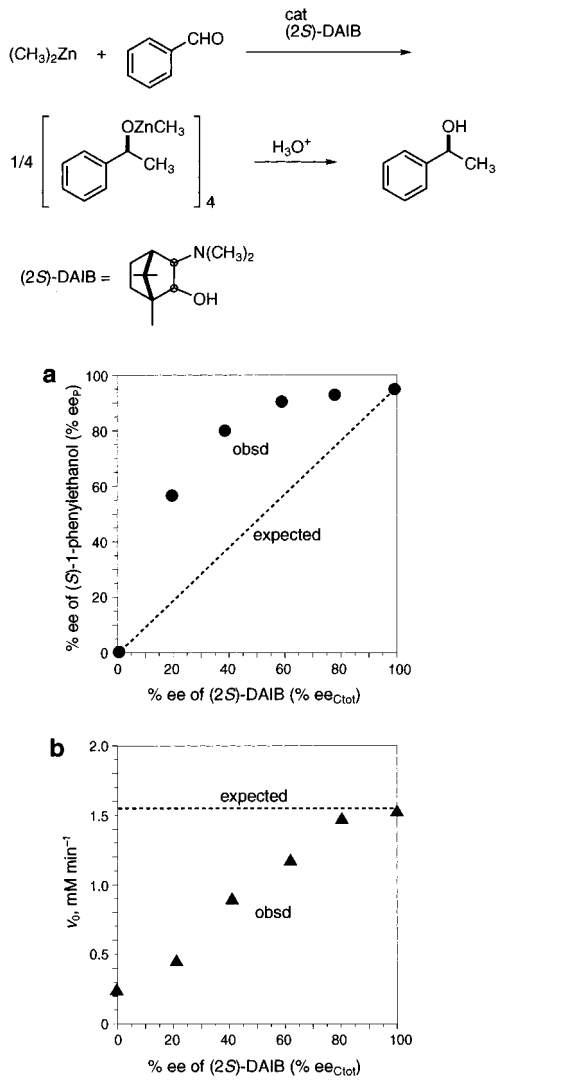

Figure 3. Nonlinear relationship between the enantiomeric purities of the product and DAIB at <30% conversion (a) and between the initial rate and DAIB ee (b) in the enantioselective methylation of benzaldehyde. Conditions: [DAIB] = 8 mM; [DMZ] = [BzH] = 420 mM; toluene; 40 °C.

Obtaining High ee$_P$ Values Using Partially Resolved DAIB. This chirality amplification is based on the difference

Scheme 2

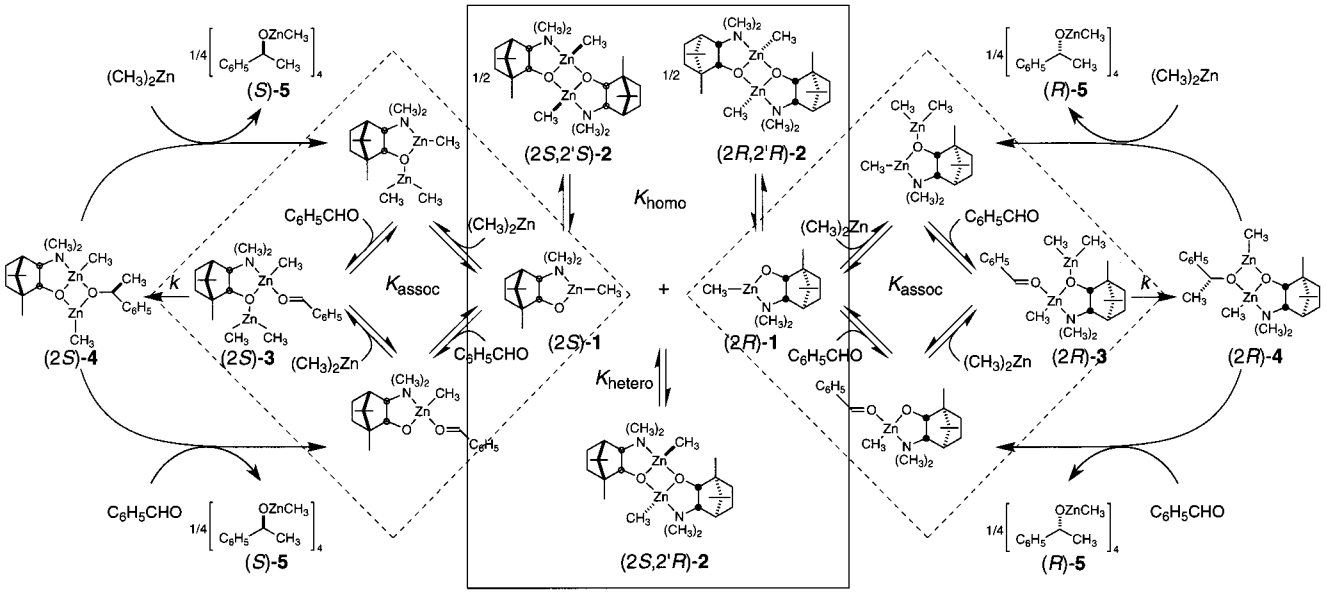

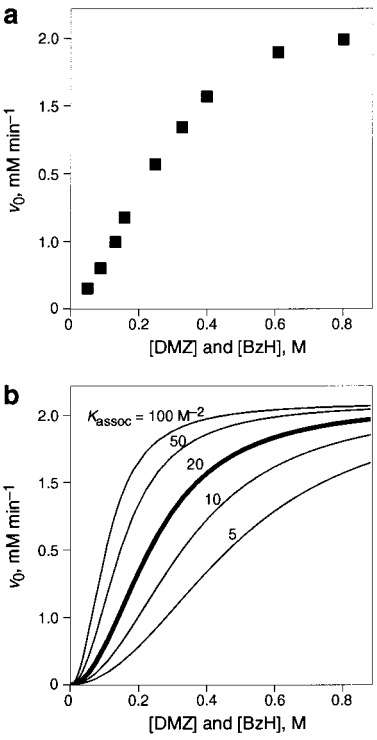

Figure 4. Determination of the rate constant k and the association constant K_{assoc}. a: Initial rate of reaction of dimethylzinc and benzaldehyde in the presence of enantiomerically pure (2*S*)-DAIB (8 mM) in toluene at 40 °C. $k = \nu_0^{sat}/[C_{tot}] = 2.5 \times 10^{-1}$ min^{-1}. b: Simulation of kinetics under the conditions, $K_{homo} = 3.0 \times 10^{-2}$ M; $K_{hetero} = 1 \times 10^{-5}$ M; $k = 2.5 \times 10^{-1}$ min^{-1}; $[C_{tot}] = 8$ mM. K_{assoc} is estimated to be 2.0×10^{1} M^{-2} by curve-fitting of graphs a and b.

in the thermodynamic stability of the homochiral and heterochiral dimers **2** (Scheme 2), where the extent of participation in the second equilibrium, forming (2*S*)- or (2*R*)-**3**, strongly influences the degree of nonlinearity. In the reaction system of Scheme 2, the enantiomeric purity of the 1-phenylethoxide is determined simply by the ratio of [(2*S*)-**3**] and [(2*R*)-**3**] and then [(2*S*)-**1**] and [(2*R*)-**1**], which are dynamically balanced through the five equilibria: 2(2*S*)-**1** ⇄ (2*S*,2′*S*)-**2**, 2(2*R*)-**1** ⇄ (2*R*,2′*R*)-**2**, (2*S*)-**1** + (2*R*)-**1** ⇄ (2*S*,2′*R*)-**2**, (2*S*)-**1** + DMZ + BzH ⇄ (2*S*)-**3**, and (2*R*)-**1** + DMZ + BzH ⇄ (2*R*)-**3**. *The high chirality amplification is realized only when dissociation of the heterochiral dimer to the racemic catalysts is insignificant.* Therefore, to gain a high degree of nonlinearity, the reaction conditions must be selected for decreasing the dissociation of (2*S*,2′*R*)-**2**.

When the concentrations of DMZ and BzH are lowered, the mixed-ligand complexes (2*S*)- and (2*R*)-**3** tend to release (2*S*)- and (2*R*)-**1**, which equilibrate with the homochiral and heterochiral dimers. The resulting higher stability of the heterochiral dimer then increases the relative amount of (2*S*)-**1** to (2*R*)-**1**, thereby enhancing the degree of nonlinearity. For example, when the reaction using an 8 mM solution of (2*S*)-DAIB in 20% ee was conducted with [DMZ] = [BzH] = 420 mM, an ee_P of only 68% was obtained. However, the ee value was increased to 80 and 89% by decreasing [DMZ] and [BzH] to 210 and to 84 mM. Figure 5a illustrates the general trend.

Second, increasing the DAIB concentration raises the concentrations of the catalyst dimers resulting in a higher chirality amplification. This is based on the tendency of even the stable heterochiral dimer to considerably dissociate to the monomers at lower concentrations. When DMZ and BzH (420 mM each) were reacted with an 8 mM concentration of DAIB in 20% ee, the methylation product was obtained in 68% ee as described above, while the reaction using a 34 mM concentration of DAIB with the same ee under otherwise identical conditions formed the adduct in 82% ee (Figure 5a). In a like manner, the ee values were improved from 82 to 94% by increasing the concentration of DAIB in 40% ee from 8 to 34 mM (Figure 5a).

Finally, changing the total concentration of the catalyst and reactants, DAIB, DMZ, and BzH, while keeping their mole ratios constant, exerts an intricate effect on the nonlinearity (Figure 6). Thus, when the reaction system with [DAIB (20% ee)] = 8 mM and [DMZ] = [BzH] = 420 mM was diluted by a factor of 3 by increasing the amount of solvent, the ee_P increased from 68 to 83%. With a 7-fold-diluted system ([DAIB] = 2.7 mM and [DMZ] = [BzH] = 140 mM to [DAIB] = 0.4 mM and [DMZ] = [BzH] = 21 mM), the ee_P value decreased from 83 to 65%. These phenomena originate from the balance of two opposite concentration effects, [DMZ] and [BzH] vs [DAIB] on ee_P. The 3-fold dilution intensifies the

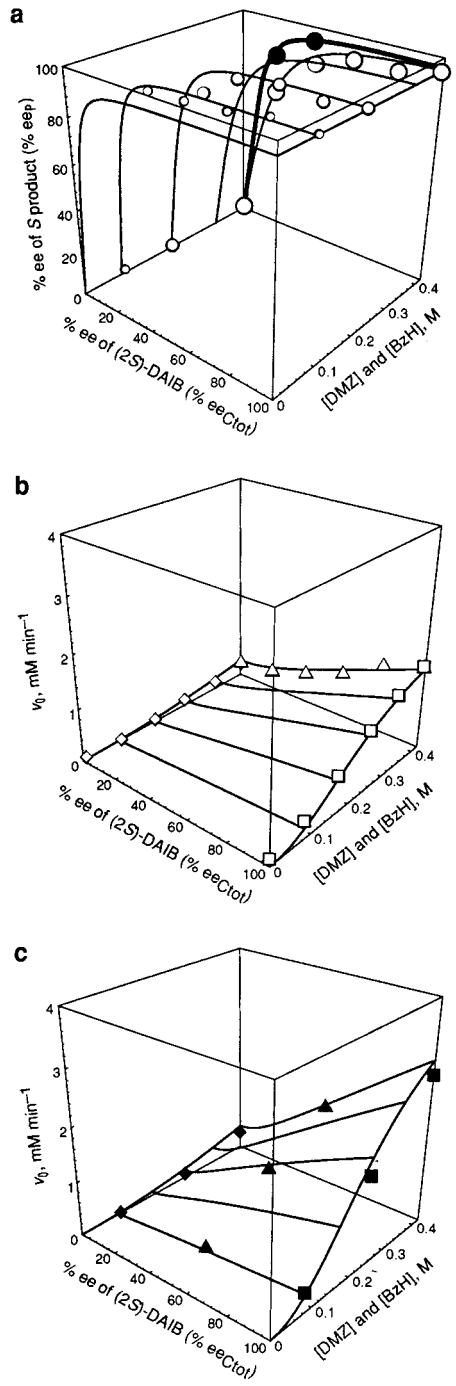

Figure 5. Simulation and observation of the nonlinear effects in the DAIB-promoted enantioselective methylation of benzaldehyde in toluene at 40 °C. a: Correlation of ee_P with ee_{Ctot} and concentration of DMZ and BzH (1:1). ∘, [DAIB] = 8 mM; [DMZ] = [BzH] = 84 mM. ○, [DAIB] = 8 mM; [DMZ] = [BzH] = 210 mM. ◯, [DAIB] = 8 mM; [DMZ] = [BzH] = 420 mM. Simulation conditions, [DAIB] = 8 mM; [DMZ] = [BzH] = 0, 84, 210, 336, 420 mM. ●, [DAIB] = 34 mM; [DMZ] = [BzH] = 420 mM. Simulation conditions, [DAIB] = 34 mM; [DMZ] = [BzH] = 420 mM. b: Correlation of v_0 with ee_{Ctot} and concentration of DMZ and BzH (1:1). □, [(2*S*)-DAIB (100% ee)] = 8 mM. ◇, [(±)-DAIB] = 8 mM. △, [DAIB] = 8 mM; [DMZ] = [BzH] = 420 mM. Simulation conditions, [DAIB] = 8 mM; [DMZ] = [BzH] = 84, 168, 252, 336, 420 mM. c: Correlation of v_0 with ee_{Ctot} and concentration of DMZ and BzH (1:1). ■, [(2*S*)-DAIB (100% ee)] = 16 mM. ◆, [(±)-DAIB = 16 mM. ▲, [(2*S*)-DAIB (50% ee)] = 16 mM. Simulation conditions, [DAIB] = 16 mM; [DMZ] = [BzH] = 84, 168, 252, 336, 420 mM. In all cases, parameters, $K_{homo} = 3.0 \times 10^{-2}$ M; $K_{hetero} = 1 \times 10^{-5}$ M; $K_{assoc} = 2.0 \times 10^{1}$ M^{-2}; $k = 2.5 \times 10^{-1}$ min^{-1}, and $ee_P^{max} = 0.95$ are used.

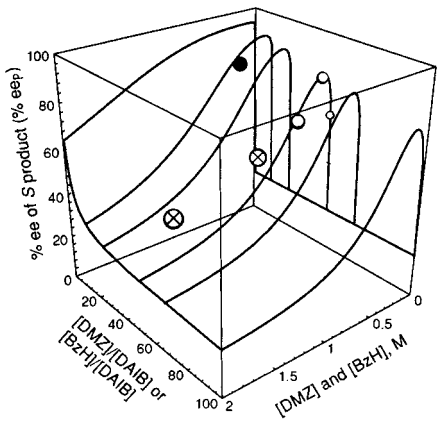

Figure 6. Correlation of ee_P with [DMZ]:[DAIB] or [BzH]:[DAIB] ratio and [DMZ] and [BzH] in the enantioselective methylation in toluene at 40 °C. Ee of (2*S*)-DAIB is fixed to 20%. ∘, [DAIB] = 0.4 mM, [DMZ] = [BzH] = 21 mM. ○, [DAIB] = 2.7 mM, [DMZ] = [BzH] = 140 mM. ◯, [DAIB] = 8 mM, [DMZ] = [BzH] = 420 mM. ⊗, [DAIB] = 16 mM, [DMZ] = [BzH] = 840 mM. ⊗, [DAIB] = 34 mM, [DMZ] = [BzH] = 1680 mM. ●, [DAIB] = 34 mM, [DMZ] = [BzH] = 420 mM. Simulation conditions, [DMZ]/[DAIB] or [BzH]/[DAIB] = 1, 12.5, 25, 50, 66.7, 100. $K_{homo} = 3.0 \times 10^{-2}$ M; $K_{hetero} = 1 \times 10^{-5}$ M; $K_{assoc} = 2.0 \times 10^{1}$ M^{-2}, and $ee_P^{max} = 0.95$. The experimental data ⊗ and ⊗ do not fit with the calculation because of [DMZ] = [BzH] ≥ 840 mM.

contribution of the unstable homochiral dimer relative to the heterochiral dimer, increasing the ee_P value. Once the limiting condition of [DAIB] = 2.7 mM where the homochiral dimer sufficiently dissociates to the monomer is reached, however, there is significant dissociation of the stable heterochiral dimer which decreases the (2*S*)-**1**:(2*R*)-**1** ratio and in turn lowers the ee_P. Figure 6 illustrates that the experimental results fit well with the simulation curves when [DMZ] = [BzH] < 840 mM (standard conditions). This can then be used to find the conditions for obtaining the highest ee_P value.

Independent vs Competitive Figures. In some asymmetric reactions that use partially resolved catalysts, a chiral and an achiral catalytic system coexist without interaction and work competitively in the same homogeneous medium. Kagan's observations in the Ti-catalyzed asymmetric oxidation of allylic alcohols or sulfides are typical examples.[3a] Here the term *f* is defined as the relative turnover efficiency of the chiral and achiral catalyst systems. In such cases, the enantiomeric ratio of the product, P_S/P_R, is determined by eq 16, where ee_P^{max} is

$$\frac{P_S}{P_R} = \frac{ee_{C_{tot}}(1 + ee_P^{max})f + (1 - ee_{C_{tot}})}{ee_{C_{tot}}(1 - ee_P^{max})f + (1 - ee_{C_{tot}})} \qquad (16)$$

the enantiomeric excess of the product obtained by an enantiomerically pure catalyst and $ee_{C_{tot}}$ is the enantiomeric excess of the catalyst used. Rearrangement of eq 16 for *f* in combination with $ee_P = (P_S - P_R)/(P_S + P_R)$ gives eq 17.

$$f = \frac{ee_P(1 - ee_{C_{tot}})}{ee_{C_{tot}}(ee_P^{max} - ee_P)} \qquad (17)$$

We attempted to analyze the enantioselectivity of the organozinc reaction in this manner. The reaction of DMZ and BzH (420 mM each) in the presence of DAIB in 20% ee (8 mM) gave the ee_P value 68%. This may be interpreted as the competition of the imaginary chiral and achiral catalytic cycles, giving the *S* alcohols in 95% ee and racemic alcohol, respec-

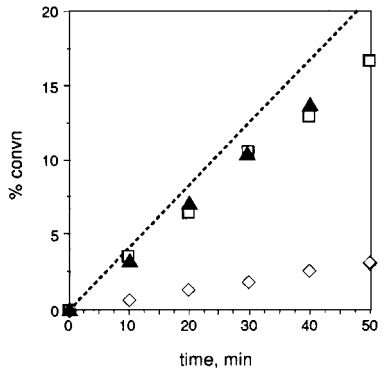

Figure 7. Conversion of the DAIB−Zn-promoted methylation of benzaldehyde in the independent and competitive systems with [DMZ] = [BzH] = 420 mM. □, [(2*S*)-DAIB (100% ee)] = 8 mM, ν_0 = 1.4 mM min^{-1}. ◇, [(±)-DAIB] = 8 mM), ν_0 = 0.22 mM min^{-1}. ▲, [(2*S*)-DAIB (50% ee)] = 16 mM ([(2*S*)-DAIB (100% ee)] = [(±)-DAIB = 8 mM, ν_0 = 1.5 mM min^{-1}. The observed rate (▲) is lower than the value expected from the operation of chiral and achiral catalytic cycles (sum of □ and ◇ given by the broken line).

tively, that coexist in a 20:80 ratio and that turn over with a 10:1 relative rate. The competitive figure, $f = 10$, is, however, different from the relative rate observed under the independent conditions; the catalysis using enantiomerically pure DAIB and the same concentrations is in fact 6.4 times faster than the reaction with racemic DAIB. With DAIB in 80% ee, the difference is further enhanced. The chiral catalyst is calculated to methylate BzH 23.5 times faster than the achiral catalyst system does. This large difference between the independent and competitive figures (6.4 vs 23.5) indicates that such an interpretation is false. The present system involves the two enantiomorphic catalytic cycles occurring at the same turnover rate (Scheme 2), and the enantiomeric purity of the product is determined simply by the ratio of the concentrations of (2*S*)- and (2*R*)-**1** in the catalytic system. The relative contribution of the *S* and *R* catalytic cycle is 5.25 with 20% ee DAIB, giving a 68% ee product, and 32.3 with 80% ee DAIB to afford the 94% ee product. The relative concentration of the monomeric catalyst is not linearly correlated with the initial ratio of (*S*)- and (*R*)-DAIB but is determined by the six parameters, K_{homo}, K_{hetero}, K_{assoc}, [DAIB], [DMZ], and [BzH].

Analysis of the reaction rate also eliminates the possibility of competition between the chiral and achiral catalytic cycles. When the coexistence of independent chiral and achiral (meso) catalytic cycles is assumed, the rate of reaction using (2*S*)-DAIB in 50% ee should be the sum of the rates of the two diastereomorphic cycles. As shown in Figure 7, however, the rate of reaction of DMZ and BzH (420 mM each) in the presence of (2*S*)-DAIB in 50% ee (16 mM; each 8 mM of chiral and racemic catalyst), indicated by ▲ is significantly less than the sum of □ and ◇ (broken line) expected from the coexistent chiral and achiral catalytic cycles. Instead, the observed reactivity is properly analyzed on the basis of the mechanism of Scheme 2. The rates of reaction with [DMZ] = [BzH] = 420 mM and [(2*S*)-DAIB (100% ee)] = 8 mM, [(±)-DAIB] = 8 mM, or [DAIB (50% ee)] = 16 mM are calculated to be 1.5, 0.32, and 1.6 mM min^{-1}, respectively. These values agree well with the experimental values. Thus, a buffer effect in the multiple equilibration system suppresses the increase in the concentration of **3** that directly correlates with the reaction rate.

Dissociative vs Associative Mechanism. The overall profile of the organozinc catalysis is fully consistent with the pathway of Scheme 2. Dissociation of the dinuclear complexes **2** generates the true catalyst **1**. Although the heterochiral system contains (2*S*,2′*R*)-**2** as the overwhelmingly major component, and at the standard 8 mM concentration, the monomers (2*S*)- and (2*R*)-**1** are present only in small quantities, the methylation reaction proceeds via the monomer **1** but not the dinuclear **2**. This view in now confirmed by the agreement between the experimentally obtained and calculated values as seen in Figures 5−7. Previously we theorized the direct participation of **2** reacting with DMZ and/or BzH.[7] The present simulation, however, excludes such an associative mechanism from consideration, at least under standard reaction conditions. Special conditions, such as higher concentrations of the catalyst, DMZ, and BzH,[17] may require serious consideration of the contribution of the associative mechanism.

Degree of Chirality Amplification as a Function of Conversion. A decrease in [DMZ] and [BzH] and an increase in [DAIB] lead to a higher degree of chirality amplification, while a limiting value exists when [DMZ] and [BzH] are varied with a fixed [DAIB]:[DMZ]:[BzH] ratio. This simulation gives excellent agreement with the experimental results at the initial stage of methylation. However, as the reaction proceeds, DMZ and BzH are consumed and the product accumulates, thereby shifting the conditions away from the initial state. In addition, product inhibition becomes nonnegligible at the later stage of the reaction, causing quantitative disagreement. There is a need for caution under such a situation.

The reaction performed with [(2*S*)-DAIB (20% ee)] = 34 mM and [DMZ] = [BzH] = 420 mM gave (*S*)-1-phenylethanol in 82% ee at 5% conversion but in 89% ee at 84% conversion. The increase in ee_P can be understood in terms of a successive decrease in [DMZ] and [BzH] (Figure 5a). The overall ee can be estimated by the integration of ee_P from time 0 to time *t* (for equations, see Supporting Information). In the highly enantioselective reaction with a high [DAIB], as shown in Figure 8a, the observed ee_P values fit well with the calculated ones even at the final stage of the reaction.

On the other hand, as shown in Figure 8b, when [DAIB (20% ee)] was reduced to 8 mM, the reaction became less enantioselective and the observed ee significantly deviates from the calculated value particularly after the middle stage. This phenomenon is explained qualitatively by assuming the product inhibition, **1** + $^1/_4$ [CH_3ZnOR^*]$_4$ [**5**, OR* = (*S*)- or (*R*)-OCH(CH_3)C_6H_5] ⇄ **4** and species derived therefrom, [**1**]$_m$[CH_3-ZnOR*]$_n$.[15] The product participation is negligible at the initial stage because of the high stability of the tetrameric alkoxide **5** as well as the existence of a large excess of DMZ and BzH.[7] During the course of methylation, however, the decrease of DMZ and BzH is accompanied by the accumulation of **5**. As a consequence, the equilibrium is shifted in the direction of **4**, and the regeneration of **3** is retarded. Thus the increase in CH_3-ZnOR* promotes the dissociation of **2**, resulting in the reduction of the chirality amplification.[18]

This process was confirmed by ^{1}H NMR experiments. The dinuclear structure of stable (2*S*,2′*R*)-**2** was not affected by the addition of an excess amount of **5** or DMZ. However, when unstable (2*S*,2′*S*)-**2** (3 mM) and (*S*)-**5** (7.5 mM) (1:5 Zn-based ratio) were mixed in toluene-d_8, catalyst/product complexes[15] were formed in 80% yield based on (2*S*,2′*S*)-**2**. The intensities of signals due to two C(2) protons of DAIB, one benzylic proton, and three Zn-methyls (−40 °C) suggested that the major

(17) Reaction with [DAIB (20% ee)] = 34 mM and [DMZ] = [BzH] = 1680 mM gave ee_P of 44% at 10% conversion, the value being higher than the expected 27% ee (Figure 6).

(18) Tetrameric (*S*)-methylzinc 1-phenylethoxide slowly catalyzes the reaction of DMZ and BzH. This effect is negligible under the standard conditions allowing smooth alkylation.

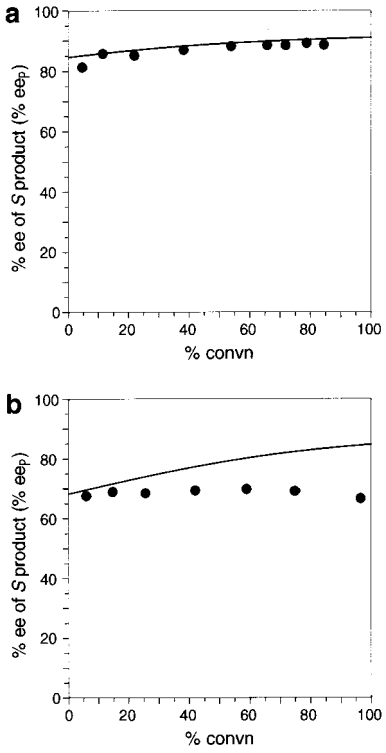

Figure 8. The ee_P conversion curve in the DAIB-promoted enantioselective methylation of benzaldehyde in toluene at 40 °C. a: [(2*S*)-DAIB (20% ee)] = 34 mM, [DMZ] = [BzH] = 420 mM. b: [(2*S*)-DAIB (20% ee)] = 8 mM, [DMZ] = [BzH] = 420 mM. Simulation conditions, $K_{homo} = 3.0 \times 10^{-2}$ M; $K_{hetero} = 1 \times 10^{-5}$ M; $K_{assoc} = 2.0 \times 10^{1}$ M^{-2}, and $ee_P^{max} = 0.95$. Line, simulation. Dot, experimental result.

product was [(2*S*)-**1**]$_2$[(*S*)-CH_3ZnOR*] with a six-membered Zn_3O_3 structure.[19] Upon the addition of 10 molar equiv of DMZ, the amounts of the new products were reduced to 30% and gave a C(2)-H signal pattern which had been obtained by mixing (2*S*,2′*S*)-**2** and DMZ in a 1:10 (Zn-based) molar ratio. Reaction of (2*S*,2′*S*)-**2** and (±)-**5**[20] gave similar diastereomeric [(2*S*)-**1**]$_m$[CH_3ZnOR*]$_n$ in 85% combined yield.[21] Here, unlike the enantiopure system, addition of 10 molar equiv of DMZ reduced the amount of these complexes to only 55%. This difference reflects the relative stabilities of (*S*)-**5** and (±)-**5**. Cryoscopic molecular weight determination showed that the aggregation state of (*S*)-**5** is 3.8, while that of (±)-**5** is 3.2,[22] indicating the lower stability of (±)-**5** compared to homochiral (*S*)-**5**. This higher tendency of nonenantiopure **5** to cause product inhibition explains the notable departure from the calculated values in the less enantioselective reaction (Figure 8b). A mixture of (2*S*,2′*S*)-**2**, (*S*)-**5**, and DMZ in a 1:10:5 Zn ratio, which approximates the conditions at ~60% conversion, gave the catalyst/product complex in ~50% yield based on (2*S*,2′*S*)-**2**. Thus, since the product inhibition becomes nonnegligible as the reaction proceeds, care must be taken to evaluate for the nonlinear effect at the late stage of reaction.

Conclusion

General equations have been developed for the quantitative treatment of nonlinear effects that result from the reversible homochiral and heterochiral dimerization of the enantiomeric catalysts. The expressions make allowance for the mechanistic interpretation of the nonlinear effects in the amino alcohol-promoted enantioselective alkylation of aldehydes. Their validity has been proven through comparison of computer-simulated graphs and experimental findings. The chirality amplification is the consequence of the combination of many structural, thermodynamic, and kinetic parameters. Most importantly, the mathematical treatment confirms that the nonlinear phenomena observed in the organozinc chemistry originate from the relative significance of the enantiomorphic cycles and not from the competition between diastereomorphic cycles involving the chiral and achiral catalysts.[23] In such asymmetric reactions, the quantitative reproduction of nonlinear effects is achievable only with identical reaction parameters, particularly concentrations of the catalyst, reagent, and substrate. Note that the reagent and substrate concentrations vary significantly in the course of reaction. The product inhibition might affect the profile as well. The detailed analysis presented in this paper, together with the earlier qualitative descriptions of the nonlinear effects,[4a,7,8] provides a logical basis for understanding the molecular mechanism of a range of chemical nonlinear phenomena.[3,4]

Experimental Section

Graphical expression of the mathematical equations in Figures 1, 2, 4, 5, 6, and 8 was aided by the Mathematica program on an Apple Macintosh computer or a Silicon Graphics computer. The key parameters, K_{homo} for the dissociation of (2*S*,2′*S*)-**2** to (2*S*)-**1** and K_{hetero} for the dissociation of (2*S*,2′*R*)-**2** to (2*S*)-**1** and (2*R*)-**1** were taken from an earlier work.[9] The DAIB-promoted asymmetric methylation of BzH with DMZ was carried out in toluene at 40 °C. The procedures for the chirality amplification experiments, kinetic studies, NMR studies, molecular weight determination, and purification of materials are essentially the same as those reported.[7,8] Commercial DMZ (Toyo Stauffer Chemical Co., Lot No. DMZ-812) was distilled at 25 °C and at 0.01 mmHg into a Schlenk tube. The purified DMZ (9.76 g, 0.102 mol) was diluted with toluene to a total volume of 30 mL under an argon stream. The resulting 3.41 M toluene solution of DMZ in a Schlenk tube equipped with a Young tap was kept at −30 °C in the dark. Solution that had been stored over 3 weeks was not used for reactions.[14] The crude (*S*)-**5** was obtained as a white solid by evaporating the volatiles from the mixture of the (*S*)-DAIB-promoted reaction [(*S*)-DAIB (111 mg, 0.564 mmol), DMZ (2.87 M toluene solution, 10.8 mL, 31.1 mmol), BzH (3.00 g, 28.2 mmol), and hexane (20 mL), 380 h]. Recrystallization from hexane (5 mL) at 0 °C gave pure (*S*)-**5** as colorless platelet crystals, mp 108−110 °C. Racemic **5** was prepared from a solution of (±)-1-phenylethanol (29.3 mg, 0.237 mmol) in hexane (2 mL) mixed with a 1.88 M DMZ solution in hexane (0.15 mL, 0.28 mmol) at 0 °C under argon atmosphere. After 24 h, all volatiles were removed under vacuum to give (±)-**5** (41.2 mg) as an oil.

The conversion was confirmed by GC using a Shimadzu GC-14A gas chromatograph:[7] The conditions (capillary column, GL Science OV-1 0.25 mm × 50 m; column temperature, 90 °C; rate of temperature increase, 2 °C min^{-1}; carrier gas, He; flow rate, 50 mL min^{-1}; split ratio, 40:1) afforded good separation of BzH and 1-phenylethanol with t_R values of 8.9 and 11.0 min, respectively. The ee of 1-phenylethanol was determined by HPLC using a Shimadzu LC-6A model under the following conditions:[7] column, Daicel Co. Chiralcel OB; eluent, 100:2 hexane/2-propanol; flow rate, 1.0 mL min^{-1}; detection, 254-nm light; t_R of the *S* isomer, 12.6 min; t_R of the *R* isomer, 18.9 min.

Chiral Amplification Experiments. (a) Effect of [DMZ] and [BzH] with a Fixed [DAIB]. [DAIB] was set to 8 mM and all reactions were stopped early. The data for 84, 210, and 420 mM DMZ and BzH are listed in the order, % ee of (2*S*)-DAIB, reaction time (min), % conversion, and % ee of (*S*)-1-phenylethanol. 84 mM: (20, 180,

(19) van der Schaaf, P. A.; Wissing, E.; Boersma, J.; Smeets, W. J. J.; Spek, A. L.; van Koten, G. *Organometallics* **1993**, *12*, 3624.

(20) Tetrameric (±)-**5** consists of (*S*)- and (*R*)-methylzinc 1-phenylethoxide in a statistical ratio.

(21) The ^{1}H NMR spectrum was more complicated than that of the homochiral system.

(22) Boersma, J. *Comprehensive Organometallic Chemistry*; Wilkinson, G.; Ed.; Pergamon Press: New York, 1982; Chapter 16.

(23) For a chemical support, see: Kitamura, M.; Oka, H.; Noyori, R. *Tetrahedron*, in press.

11.2, 88.9), (40, 180, 26.6, 88.7), (60, 180, 30.6, 92.3), (80, 120, 26.3, 95.9), (100, 100, 25.4, 95.7). 210 mM: (20, 160, 11.8, 80.1), (40, 180, 23.0, 93.3), (60, 180, 29.7, 92.5), (80, 160, 23.8, 92.6), (100, 75, 27.9, 94.9). 420 mM: (20, 120, 6.3, 67.6), (40, 80, 6.0, 82.2), (60, 80, 17.6, 89.8), (80, 40, 13.6, 93.9), (100, 30, 17.2, 94.5).

(b) Effect of [DAIB] with a Fixed [DMZ] and [BzH]. [DMZ] and [BzH] were set to 420 mM. For [DAIB (20% ee)] = 8 mM and [DAIB (40% ee)] = 8 mM, the data from experiment a was used. For [DAIB] = 34 mM the data are listed in the order of reaction time (min), % conversion, and % ee of (*S*)-1-phenylethanol. (2*S*)-DAIB in 20% ee: (20, 5.1, 81.6). (2*S*)-DAIB in 40% ee: (20, 16.0, 94.1).

(c) Effect of Total Concentration with a Fixed [DAIB]:[DMZ]:[BzH] Ratio. The ee of (2*S*)-DAIB was set to 20%. The collected data are listed in the order of [DAIB] (mM), [DMZ] and [BzH] (mM), reaction time (min), % conversion, and % ee of (*S*)-1-phenylethanol. [DAIB]:[DMZ]:[BzH] = 1:50:50: (0.4, 21, 140, 2.3, 64.6), (2.7, 140, 180, 5.0, 83.1), (16, 840, 30, 3.7, 56.5), (34, 1680, 30, 10.0, 44.3). [DAIB]:[DMZ]:[BzH] = 1:12.5:12.5: (34, 420, 20, 5.1, 81.6).

(d) Effect of the Conversion on the Degree of Chirality Amplification. The data are listed in the order of reaction time (min), % conversion, and % ee of (*S*)-1-phenylethanol. [DAIB (20% ee)] = 34 mM and [DMZ] = [BzH] = 420 mM: (20, 5.1, 81.6), (40, 11.6, 85.8), (85, 22.1, 85.2), (175, 38.3, 87.1), (320, 54.1, 88.3), (495, 66.0, 88.7), (765, 72.2, 88.6), (1400, 79.3, 89.7), (3305, 84.5, 89.0). [DAIB (20% ee)] = 8 mM and [DMZ] = [BzH] = 420 mM: (120, 6.3, 67.6), (240, 14.5, 68.3), (480, 25.5, 68.3), (910, 42.2, 69.2), (1530, 59.2, 70.1), (2840, 75.4, 69.1), (20000, 96.8, 66.4).

Kinetic Studies. (a) v_0 to ([DMZ] and [BzH]) Relationship Using Optically Pure DAIB. The kinetic experiments using 8 mM (2*S*)-DAIB in 100% ee were conducted by varying [DMZ] or [BzH] over a range of 42−840 mM with a fixed 1:1 DMZ to BzH ratio. The time−conversion relationship and the initial rates are listed for each concentration of DMZ and BzH. 42 mM: (20, 4.0), (40, 11.5), (60, 15.8), (80, 22.1), (100, 25.3), (120, 30.5); 0.28% min^{-1} = 0.12 mM min^{-1}. 84 mM: (20, 4.7), (40, 13.5), (60, 18.5), (80, 27.7), (100, 32.1), (120, 34.4); 0.34% min^{-1} = 0.29 mM min^{-1}. 126 mM: (20, 6.0), (40, 15.0), (60, 23.6), (80, 30.0), (100, 36.2), (120, 41.7); 0.38% min^{-1} = 0.48 mM min^{-1}. 168 mM: (20, 7.1), (40, 14.5), (60, 22.8), (80, 29.0), (100, 35.0), (120, 40.6); 0.39% min^{-1} = 0.65 mM min^{-1}. 252 mM: (20, 7.5), (40, 17.1), (60, 24.4), (80, 32.2), (100, 37.8), (120, 43.6); 0.42% min^{-1} = 1.1 mM min^{-1}. 336 mM: (20, 9.0), (40, 16.9), (60, 25.8), (80, 32.1), (100, 40.0), (120, 45.3); 0.40% min^{-1} = 1.4 mM min^{-1}. 420 mM: (10, 3.5), (20, 6.6), (30, 10.8), (40, 13.2), (50, 16.9), (60, 20.0); 0.33% min^{-1} = 1.4 mM min^{-1}. 630 mM: (20, 6.1), (40, 13.5), (60, 19.9), (80, 25.5), (100, 31.9), (120, 37.3); 0.30% min^{-1} = 1.9 mM min^{-1}. 840 mM: (20, 4.5), (40, 10.2), (60, 15.3), (80, 20.3), (100, 25.0), (120, 30.2); 0.24% min^{-1} = 2.0 mM min^{-1}. These data was used to determine the rate constant k and the association constant K_{assoc}.

(b) v_0 to ([DMZ] and [BzH]) Relation Using Racemic DAIB. All the collected time−conversion data obtained with 8 mM of (±)-DAIB by varying [DMZ] or [BzH] over a range of 84−420 mM with a fixed 1:1 DMZ to BzH ratio are listed. 84 mM: (120, 1.7), (180, 2.1), (240, 2.9), (300, 3.9), (360, 4.5); 0.012% min^{-1} = 0.010 mM min^{-1}. 168 mM: (60, 1.9), (120, 3.5), (180, 5.4), (240, 7.4), (300, 8.5), (360, 11.7); 0.031% min^{-1} = 0.052 mM min^{-1}. 252 mM: (60, 2.9), (120, 5.2), (180, 8.1), (240, 10.8); 0.045% min^{-1} = 0.11 mM min^{-1}. 336 mM: (60, 2.9), (120, 5.8), (180, 8.5), (240, 10.5); 0.047% min^{-1} = 0.16 mM min^{-1}. 420 mM: (10, 0.58), (20, 1.2), (30, 1.7), (40, 2.5), (50, 3.1), (60, 3.8), (120, 7.1), (180, 9.8), (240, 12.5), (300, 16.1); 0.053% min^{-1} = 0.22 mM min^{-1}.

(c) Relation between v_0, ee_{Ctot}, and [DMZ] and [BzH]. The correlation between v_0 and ee of (2*S*)-DAIB was deduced from the results obtained under the following conditions: 8 mM (2*S*)-DAIB in 0, 20, 40, 60, 80, and 100% ee; [DMZ] = [BzH] = 420 mM. The original data for the time−conversion relationship and the initial rates are listed. 0% ee: (10, 0.58), (20, 1.2), (30, 1.7), (40, 2.5), (50, 3.1), (60, 3.8), (120, 7.1), (180, 9.8), (240, 12.5), (300, 16.1); 0.053% min^{-1} = 0.22 mM min^{-1}. 20% ee: (60, 4.0), (120, 8.5), (180, 13.4), (240, 17.5), (300, 21.3), (360, 24.5), (420, 26.5); 0.074% min^{-1} = 0.31 mM min^{-1}. 40% ee: (60, 8.1), (120, 16.6), (180, 25.1), (240, 32.2), (300, 37.6), (360, 41.2); 0.14% min^{-1} = 0.59 mM min^{-1}. 60% ee: (40, 8.4), (80, 16.9), (120, 25.1), (160, 32.9), (200, 38.9), (240, 45.0); 0.21% min^{-1} = 0.88 mM min^{-1}. 80% ee: (20, 6.1), (40, 12.2), (60, 18.9), (80, 24.6), (100, 29.8), (120, 37.4); 0.32% min^{-1} = 1.3 mM min^{-1}. 100% ee: (10, 3.5), (20, 6.6), (30, 10.8), (40, 13.2), (50, 16.9), (60, 20.0); 0.33% min^{-1} = 1.4 mM min^{-1}.

The correlation between v_0 and ee of (2*S*)-DAIB with [DAIB] = 16 mM was deduced from the results obtained under the following conditions: (2*S*)-DAIB in 0, 50, and 100% ee; [DMZ] = [BzH] = 84, 252, and 420 mM. The original data for the time-conversion relationship and the initial rates are listed. [DMZ] = [BzH] = 84 mM: 0% ee: (120, 1.9), (180, 2.7), (240, 4.6), (300, 5.3), (360, 5.9); 0.017% min^{-1} = 0.014 mM min^{-1}. 50% ee: (15, 4.6), (30, 8.0), (45, 8.2), (60, 15.9), (75, 19.6), (90, 22.2); 0.25% min^{-1} = 0.21 mM min^{-1}. 100% ee: (15, 7.2), (30, 13.7), (45, 21.3), (60, 26.6), (75, 29.0), (90, 34.6); 0.38% min^{-1} = 0.32 mM min^{-1}. [DMZ] = [BzH] = 252 mM: 0% ee: (80, 3.2), (120, 4.6), (160, 5.0), (200, 8.5), (240, 12.7); 0.049% min^{-1} = 0.12 mM min^{-1}. 50% ee: (15, 5.3), (30, 11.3), (45, 16.8), (60, 23.5), (75, 28.9), (90, 32.3); 0.37% min^{-1} = 0.94 mM min^{-1}. 100% ee: (10, 5.2), (25, 15.0), (35, 20.3), (45, 26.3), (55, 34.4), (70, 41.8); 0.61% min^{-1} = 1.5 mM min^{-1}. [DMZ] = [BzH] = 420 mM: 0% ee: (40, 1.7), (80, 4.7), (120, 6.9), (160, 12.2), (200, 13.6), (240, 18.0); 0.076% min^{-1} = 0.32 mM min^{-1}. 50% ee: (10, 3.2), (20, 6.8), (30, 10.6), (40, 13.5), (60, 19.6), (80, 25.3), (100, 30.2), (120, 34.6), (180, 45.4); 0.35% min^{-1} = 1.5 mM min^{-1}. 100% ee: (10, 6.8), (20, 13.8), (30, 20.5), (40, 26.2), (50, 32.3), (60, 38.8); 0.64% min^{-1} = 2.7 mM min^{-1}.

Determination of Aggregation States of 5. The molecular weights of (*S*)-**5** and (±)-**5**[20] were determined by depression of the freezing point in benzene solution according to the reported procedure.[7] A standard freezing point depression apparatus was used, equipped with a sidearm through which the cell could be connected to a dual-manifold vacuum/argon system. Molecular weight was calculated in each case from $\Delta T = K_f\omega/MW$, where ΔT is the depression (degrees), K_f is the molar depression of the solvent, ω is the weight (g) of solute in 1000 g of solvent, and MW is molecular weight. The K_f value of this apparatus was calculated to be 5.16 on the basis of the depression of a benzene (10.53 g) solution by naphthalene (118.6−566.6 mg). The averaged ΔT values for (*S*)-**5** and (±)-**5** obtained from four runs were 0.318 and 0.37 (0.35−0.39), respectively. The molecular weights of (*S*)-**5** and (±)-**5** were calculated to be 759 and 647 (620−690), indicating the aggregation state to be 3.8 and 3.2, respectively.

Acknowledgment. We thank Professor H. Suga (Osaka University) for suggestions and encouragement. We also acknowledge Mr. Y. Takezawa, Wolfram Research, Inc., for his quick and kind technical suggestion for the use of the Mathematica program. This work was aided by Grand-in-Aid for COE Research (07CE2004) from the Ministry of Education, Science, Sports and Culture, Japan.

Supporting Information Available: Induction of equations for graphical expression of Figures 4b, 5b, 6, and 8 as well as ^{1}H NMR experiments (5 pages, print/PDF). See any current masthead page for ordering information and Web access instructions.

JA981740Z